

---

# Ensembling Sparse Autoencoders

---

**Soham Gadgil\***

University of Washington  
sgadgil@cs.washington.edu

**Chris Lin\***

University of Washington  
clin25@cs.washington.edu

**Su-In Lee**

University of Washington  
suinlee@cs.washington.edu

## Abstract

Sparse autoencoders (SAEs) are used to decompose neural network activations into human-interpretable features. Typically, features learned by a single SAE are used for downstream applications. However, it has recently been shown that SAEs trained with different initial weights can learn different features, demonstrating that a single SAE captures only a limited subset of features that can be extracted from the activation space. Motivated by this limitation, we propose to ensemble multiple SAEs through *naive bagging* and *boosting*. Specifically, SAEs trained with different weight initializations are ensembled in naive bagging, whereas SAEs sequentially trained to minimize the residual error are ensembled in boosting. We evaluate our ensemble approaches with three settings of language models and SAE architectures. Our empirical results demonstrate that ensembling SAEs can improve the reconstruction of language model activations, diversity of features, and SAE stability. Furthermore, ensembling SAEs performs better than applying a single SAE on downstream tasks such as concept detection and spurious correlation removal, showing improved practical utility.

## 1 Introduction

Sparse autoencoders (SAEs) have been shown to decompose neural network activations<sup>2</sup> into a high-dimensional and sparse space of human-interpretable features [8, 19, 27, 33]. Recent work has focused on the application of SAEs to language models with interpretability use cases such as detecting concepts [19, 29], identifying internal mechanisms of model behaviors [28], and steering model behaviors [13, 28, 31]. In practice, given a set of activations, a single SAE is usually selected for downstream interpretability applications. However, it has recently been shown that SAEs trained on the same activations learn different features while differing only in their initial weights [15, 32]. This suggests that, even with the same architecture and hyperparameters, each SAE captures a different and yet limited subset of features that can be extracted from the activation space. This variability can be viewed as a limitation of SAEs that undermines their reliability, and SAE architectures with additional constraints have been proposed to address the instability of SAEs [15].

Here, we offer a different perspective by asking: *Can we leverage the variability of SAEs to improve performance?* This perspective is motivated by ensemble methods in supervised learning that leverage model variability to improve predictive performance, with classical examples such as bagging (bootstrap aggregating) [2, 3] and boosting [7, 17]. Therefore, we propose to ensemble multiple SAEs and instantiate two approaches (Figure 1). First, in *naive bagging*, SAEs differing only

---

\*Equal contribution.

<sup>2</sup>Activations from neural networks are often also described as embeddings or representations.

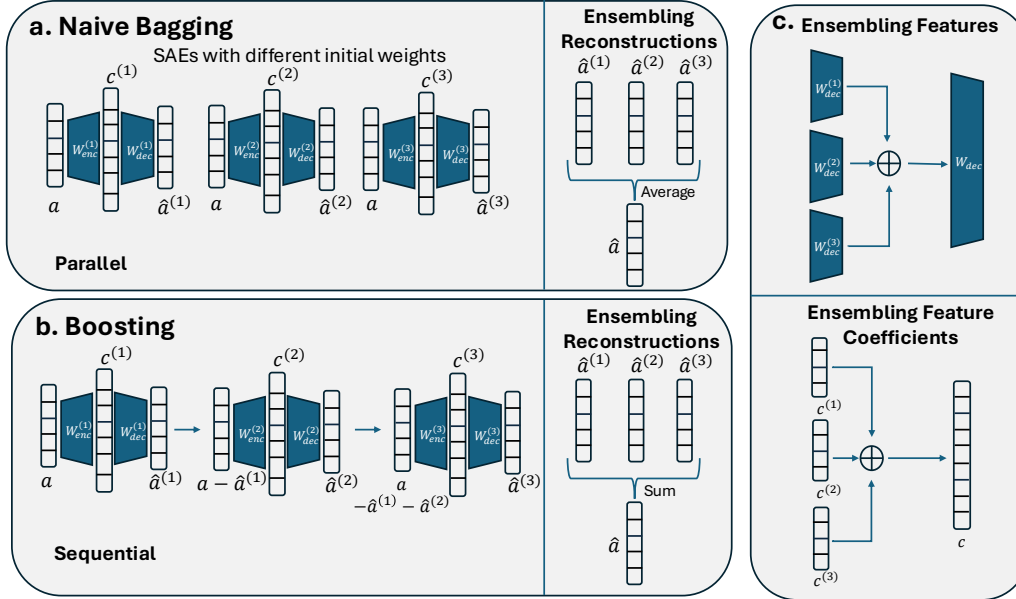


Figure 1: Overview of the proposed SAE ensembling strategies. **a.** *Naive Bagging* involves multiple SAEs with different weight initializations, which can be trained in parallel. The ensembled reconstruction is the average of reconstructions obtained from each individual SAE. **b.** *Boosting* involves sequential training of SAEs on the residual error left from the previous iterations. The ensembled reconstruction is the sum of the reconstructions of the individual SAEs. **c.** For both approaches, ensembling the features and feature coefficients involves a concatenation.

in their weight initializations are ensembled. Second, in *boosting*, the ensemble aggregates SAEs that are iteratively trained to reconstruct the residual from previous iterations. Conceptually, naive bagging and boosting of SAEs are motivated as methods for ensembling the outputs of SAEs in the activation space. Nevertheless, we show that ensembling the outputs of SAEs corresponds to concatenating the SAE features. In three settings of language models and SAE architectures, our empirical results show that naive bagging and boosting can lead to better reconstruction of language model activations, more diverse features, and better stability. Finally, to demonstrate the practical utility of our ensemble methods, we apply them to the tasks of concept detection and spurious correlation removal, where ensembling multiple SAEs outperforms using only one SAE.

## 2 Related Work

**SAEs.** SAEs have emerged as a scalable and unsupervised approach for extracting human-interpretable features from neural network activations [8, 14], with recent work demonstrating their applications to language models [19, 27]. An SAE decomposes neural network activations into sparse linear combinations of features, which are vectors with the same dimensionality as the original activations. Overall, features learned by an SAE can often be annotated with semantic interpretations [8, 35]. Because the immediate goal of training an SAE is to decompose activations into sparse combinations of features, intrinsic metrics such as the explained variance of reconstructions and feature sparsity are used to evaluate SAEs [19, 33, 34]. At the same time, SAEs are usually trained with the end goal of interpreting language model behaviors, with downstream use cases such as concept detection [19, 29], mechanistic interpretability [28], and model steering [13, 28, 31]. Therefore, metrics specific to downstream applications such as concept detection accuracy and the SHIFT score have been proposed [23].

**Variability of SAEs.** In general, the variability of SAEs can come from several sources. First, SAEs with different architecture designs can learn different features. For example, it has been shown that the choice of SAE activation function corresponds to assumptions about the separability structure of the features to be learned [21]. The SAE size also has an impact on the types of features learned—a smaller SAE tends to learn high-level features, while a larger SAE tends to learn more specific

features [6]. Architectural variants such as SAE stitching and Matryoshka SAE allow features with various degrees of specificity to be incorporated at the same time [5, 26]. Second, given a fixed architecture, SAEs with different training hyperparameters can also learn different features. For example, it has been found that lower learning rates can help reduce the number of dead features that rarely activate [19]. Finally, it has been shown that SAEs can learn different features even with the same architecture and hyperparameters, for example due to different initial weights [15, 32]. For the scope of this paper, we focus on the variability and ensembling of SAEs with the same architecture and hyperparameters. In other words, our SAE ensemble approaches are considered meta-algorithms compatible with any SAE architecture and hyperparameter configuration.

**Model ensembling.** Ensemble methods have been applied to leverage model variability for improving performance, especially in supervised learning. In bagging (bootstrap aggregating), predictions from models trained with bootstrapped data subsets are aggregated [2, 3]. Boosting algorithms train successive models by focusing on the errors made in the previous iterations [7, 17]. Stacking is an alternative framework that combines predictions from models with different architectures and inductive biases [36]. More recently, it has been shown that averaging weights of models can lead to improved accuracy without additional inference time [37, 38]. For unsupervised learning, ensemble methods have mostly been applied to form consensus for clustering and anomaly detection [1, 11, 16, 20, 40]. Motivated by the principle of ensembling, here we propose that SAEs can also be ensembled with respect to their outputs in the activation space. We show that ensembling SAE reconstructions corresponds to combining SAE features. Furthermore, we demonstrate that ensembling SAEs can lead to improved intrinsic performance and practical utility when applied to language models.

Overall, our work makes the following contributions. (1) We propose ensembling SAEs as a framework to leverage the variability of SAEs and instantiate two specific approaches, naive bagging and boosting of SAEs, with theoretical justifications in relation to reconstruction performance. (2) We show that ensembling of the output SAE reconstructions is equivalent to ensembling the SAE features. (3) We empirically demonstrate that ensembling multiple SAEs (trained on language model activations), compared to training a single SAE, can lead to better performance in intrinsic metrics and downstream applications.

### 3 Preliminaries

This section provides the notation used throughout this paper, the definition of an SAE ensemble, and a theoretical result showing that ensembling SAEs is equivalent to concatenating their features.

#### 3.1 Notation

In general, we consider a neural network that maps from a sample space  $\mathcal{X}$  to a  $d$ -dimensional activation space. An SAE is an autoencoder  $g : \mathbb{R}^d \rightarrow \mathbb{R}^d$  that reconstructs neural network activations, with the following form:

$$g(\mathbf{a}; \mathbf{W}_{\text{enc}}, \mathbf{W}_{\text{dec}}, \mathbf{b}_{\text{enc}}, \mathbf{b}_{\text{dec}}) = \mathbf{W}_{\text{dec}} h(\mathbf{W}_{\text{enc}} \mathbf{a} + \mathbf{b}_{\text{enc}}) + \mathbf{b}_{\text{dec}}, \quad (1)$$

where  $\mathbf{W}_{\text{enc}} \in \mathbb{R}^{k \times d}$ ,  $\mathbf{b}_{\text{enc}} \in \mathbb{R}^k$ ,  $\mathbf{W}_{\text{dec}} \in \mathbb{R}^{d \times k}$ ,  $\mathbf{b}_{\text{dec}} \in \mathbb{R}^d$  are the SAE weights and biases, and  $h : \mathbb{R}^k \rightarrow \mathbb{R}^k$  is an element-wise activation function such as the ReLU, JumpReLU, and TopK functions [8, 19, 27]. In contrast to conventional autoencoders, in an SAE we have  $k > d$ . Notably, the columns of the decoder matrix  $\mathbf{W}_{\text{dec}}$  are considered features learned by the SAE. Particularly, let  $\mathbf{W}_{\text{dec}}[:, i]$  denote the  $i$ th column of the decoder matrix. Then  $\mathbf{f}_i = \mathbf{W}_{\text{dec}}[:, i] \in \mathbb{R}^d$  is the  $i$ th feature of the SAE, for  $i \in [k]$ .<sup>3</sup> Furthermore, elements in  $\mathbf{c} = h(\mathbf{W}_{\text{enc}} \mathbf{a} + \mathbf{b}_{\text{enc}}) \in \mathbb{R}^k$  are considered coefficients for the features. Overall, Equation (1) can be rewritten to highlight that an SAE decomposes an activation into features, as follows:

$$g(\mathbf{a}; \mathbf{W}_{\text{enc}}, \mathbf{W}_{\text{dec}}, \mathbf{b}_{\text{enc}}, \mathbf{b}_{\text{dec}}) = \sum_{i=1}^k \mathbf{c}_i \mathbf{f}_i + \mathbf{b}_{\text{dec}}. \quad (2)$$

For conciseness, we let  $\theta = (\mathbf{W}_{\text{enc}}, \mathbf{W}_{\text{dec}}, \mathbf{b}_{\text{enc}}, \mathbf{b}_{\text{dec}})$  denote all the SAE parameters. Finally, we use  $\hat{\mathbf{a}} = g(\mathbf{a}; \theta)$  to denote the SAE reconstruction.

<sup>3</sup>Throughout this paper,  $[B] = \{1, \dots, B\}$  for any positive integer  $B$ .

To train an SAE, a training set of activations  $\{\mathbf{a}^{(n)}\}_{n=1}^N$  are collected by passing a set of samples  $\{\mathbf{x}^{(n)}\}_{n=1}^N$  through the neural network. Then the SAE parameters are trained to minimize the following empirical loss:

$$\mathcal{L}_{\text{SAE}}\left(\{\mathbf{a}^{(n)}\}_{n=1}^N; \theta\right) = \frac{1}{N} \sum_{n=1}^N \left[ \underbrace{\left\| \mathbf{a}^{(n)} - g\left(\mathbf{a}^{(n)}; \theta\right) \right\|_2^2}_{\text{reconstruction loss}} + \lambda \underbrace{\left\| \mathbf{c}^{(n)} \right\|_p}_{\text{sparsity loss}} \right], \quad (3)$$

where  $\mathbf{c}^{(n)} = h(\mathbf{W}_{\text{enc}}\mathbf{a}^{(n)} + \mathbf{b}_{\text{enc}})$  corresponds to the feature coefficients for the  $n$ th sample, and  $\lambda \geq 0$  is the penalty coefficient for the sparsity loss. In particular,  $\lambda = 0$  for TopK SAE because the number of non-zero feature coefficients is directly controlled [19],  $p = 0$  for JumpReLU SAE [34], and  $p = 1$  for ReLU and Gated SAEs [8, 33].

### 3.2 Ensembling SAEs

In this work we focus on ensembling SAEs with the same architecture. Specifically, given  $J$  SAEs with model parameters  $\theta^{(j)}$  for  $j \in [J]$ , an SAE ensemble has the form:

$$\sum_{j=1}^J \alpha^{(j)} g\left(\cdot; \theta^{(j)}\right) \quad (4)$$

, where  $\alpha^{(j)} \geq 0$  is the ensemble weight for the  $j$ th SAE, and for generality the notation  $g(\cdot; \theta^{(j)})$  indicates that each SAE can take arbitrary inputs in  $\mathbb{R}^d$ . This weighted-sum formulation is similar to classical ensemble methods, where a weighted sum of outputs from base models is used to make a prediction [2, 17]. With an SAE ensemble, the base models are now SAEs. Interestingly, because the output of each SAE is a linear combination of its features, ensembling SAEs is equivalent to concatenating their feature coefficients and their decoder matrices (feature vectors). More formally, we have the following proposition, with the proof in Appendix A.

**Proposition 1.** *Suppose there are  $J$  SAEs  $g(\cdot; \theta^{(1)}), \dots, g(\cdot; \theta^{(J)})$ , with decoder matrices  $\mathbf{W}_{\text{dec}}^{(1)}, \dots, \mathbf{W}_{\text{dec}}^{(J)} \in \mathbb{R}^{d \times k}$  and decoder biases  $\mathbf{b}_{\text{dec}}^{(1)}, \dots, \mathbf{b}_{\text{dec}}^{(J)} \in \mathbb{R}^d$ . For a given neural network activation  $\mathbf{a} \in \mathbb{R}^d$ , let  $\mathbf{c}^{(1)}, \dots, \mathbf{c}^{(J)} \in \mathbb{R}^k$  denote the feature coefficients. Then ensembling the  $J$  SAEs is equivalent to reconstructing  $\mathbf{a}$  with:*

$$\hat{\mathbf{a}} = \mathbf{W}_{\text{dec}} \mathbf{c} + \mathbf{b}_{\text{dec}} = \sum_{i'=1}^{kJ} \mathbf{c}_{i'} \mathbf{f}_{i'} + \mathbf{b}_{\text{dec}}, \quad (5)$$

where

$$\mathbf{c} = \begin{bmatrix} \alpha^{(1)} \mathbf{c}^{(1)} \\ \vdots \\ \alpha^{(J)} \mathbf{c}^{(J)} \end{bmatrix}, \mathbf{W}_{\text{dec}} = [\mathbf{W}_{\text{dec}}^{(1)} \dots \mathbf{W}_{\text{dec}}^{(J)}], \mathbf{b}_{\text{dec}} = \sum_{j=1}^J \alpha^{(j)} \mathbf{b}_{\text{dec}}^{(j)}, \quad (6)$$

and  $\mathbf{f}_{i'} = \mathbf{W}_{\text{dec}}[:, i']$ , with  $\mathbf{c} \in \mathbb{R}^{kJ}$ ,  $\mathbf{W}_{\text{dec}} \in \mathbb{R}^{d \times kJ}$ ,  $\mathbf{b}_{\text{dec}} \in \mathbb{R}^d$ .

**Remark 1.** The ensemble weights  $\{\alpha^{(j)}\}_{j=1}^J$  can be folded into either  $\mathbf{c}$  or  $\mathbf{W}_{\text{enc}}$  for Proposition 1 to hold. Since the columns of  $\mathbf{W}_{\text{dec}}$  are often constrained to have unit norms to interpret the features as direction vectors [8, 33], the ensemble weights are folded into  $\mathbf{c}$  to retain the feature norms.

## 4 Ensemble Methods for SAEs

In this section we describe *naive bagging* and *boosting* as two approaches for ensembling SAEs.

### 4.1 Naive Bagging

Variability of SAEs due to weight initialization is utilized in naive bagging, motivated by prior work showing that SAEs differing only in their initial weights can learn different features [15, 32]. Note that we refer to this method as *naive* because, unlike classical bagging, bootstrapped data subsets are not

used. This is to ensure that each SAE is trained on the same dataset and isolate the effect of different initializations. Also, as SAEs are often trained on million- or even billion-scale datasets [19, 27], bootstrapping becomes impractical due to memory and storage overhead. Concretely, given  $J$  SAEs with different initial weights, naive bagging gives the following ensembled SAE:

$$g_{\text{NB}}(\mathbf{a}^{(*)}; \{\theta^{(j)}\}_{j=1}^J) = \frac{1}{J} \sum_{j=1}^J g(\mathbf{a}^{(*)}; \theta^{(j)}) \quad (7)$$

Conceptually, the uniform ensemble weight  $\alpha^{(j)} = 1/J$  is motivated by considering naive bagging as a way to reduce reconstruction variance in the bias-variance decomposition (see Proposition 2 in Appendix A for a formal justification).

## 4.2 Boosting

Since SAEs with different initial weights still learn some overlapping features [32], naive bagging can result in redundant features in the ensemble. To address this redundancy, we propose a boosting-based ensemble strategy to encourage SAEs to capture different components of a given activation through sequential training. Starting from a base SAE, each subsequent SAE is trained to capture the residual left from the previous iteration. Concretely, the  $j$ th SAE is trained with the following loss:

$$\mathcal{L}_{\text{Boost}}(\{\mathbf{a}^{(n)}\}_{n=1}^N; \theta^{(j)}) = \frac{1}{N} \sum_{n=1}^N \left[ \left\| \mathbf{a}^{(n,j)} - g(\mathbf{a}^{(n,j)}; \theta^{(j)}) \right\|_2^2 + \lambda \left\| \mathbf{c}^{(n,j)} \right\|_p \right], \quad (8)$$

where

$$\mathbf{a}^{(n,j)} = \begin{cases} \mathbf{a}^{(n)}, & \text{if } j = 1. \\ \mathbf{a}^{(n)} - \sum_{\ell=1}^{j-1} g(\mathbf{a}^{(n,\ell)}; \theta^{(\ell)}), & \text{otherwise.} \end{cases}$$

Here, the first iteration corresponds to training the base SAE with the original activations. For  $j > 1$ ,  $\mathbf{a}^{(n,j)}$  is the residual left from the  $(j - 1)$ th iteration that the  $j$ th SAE should learn to reconstruct. It is worth noting that the regularization parameters  $\lambda$  and  $p$  remain the same throughout the training iterations. Intuitively, each SAE in boosting should learn features different from the previous SAEs by capturing the residual. As another motivation, boosting can also lead to good reconstruction performance by bounding the bias term in the bias-variance decomposition (see Proposition 3 in Appendix A for a formal justification). Overall, given  $J$  SAEs trained with Equation (8), boosting gives the following ensembled SAE:

$$g_{\text{Boost}}(\mathbf{a}^{(*)}; \{\theta^{(j)}\}_{j=1}^J) = \sum_{j=1}^J g(\mathbf{a}^{(*,j)}; \theta^{(j)}). \quad (9)$$

## 5 Experiments

In this section, we quantitatively evaluate our ensemble approaches with intrinsic evaluation metrics (Section 5.1) and demonstrate the utility of ensembling SAEs with two use cases (Section 5.2 and Section 5.3).

### 5.1 Evaluating Ensembled SAEs with Intrinsic Metrics

#### 5.1.1 Setup

We evaluate our ensemble approaches on SAEs trained with activations from three different language models: GELU-1L, Pythia-160M, and Gemma 2-2B, which represent a range of model sizes. Following prior work, ReLU, TopK, and JumpReLU SAEs are trained with the residual stream activations from GELU-1L [4], layer 8 from Pythia-160M [19], and layer 12 from Gemma 2-2B [27], respectively. Per-token activations are obtained from the Pile [18] for each language model with the corresponding context size. For training the SAEs, we use 800 million tokens from a version of the Pile with copyrighted contents removed.<sup>4</sup> A held-out test set of 7 million tokens is used for

<sup>4</sup><https://huggingface.co/datasets/monology/pile-uncopyrighted>

evaluation. For each set of language model and SAE architecture, hyperparameters are swept for the base SAE, and hyperparameters giving an explained variance closest to 90% are selected. This ensures that the SAEs being ensembled are practically usable to explain the activations. All SAEs are trained using the Adam optimizer [24]. Additional details about the language models along with training times and hyperparameter selection are provided in Appendix D.

### 5.1.2 Metrics

We evaluate different aspects of the ensembled SAEs using six different intrinsic metrics. Here  $N$  refers to the total number of per-token activations used for evaluation, and  $m$  the total number of SAE features (e.g.  $m = kJ$  for ensembled SAEs and  $m = k$  for a single SAE).

**Reconstruction performance.** We use two standard metrics, mean squared error (MSE) and explained variance, to evaluate the reconstruction of activations:

$$\text{MSE} = \frac{1}{N} \sum_{n=1}^N \left\| \mathbf{a}^{(n)} - \hat{\mathbf{a}}^{(n)} \right\|_2^2, \text{ and}$$

$$\text{Explained Variance} = \frac{1}{d} \sum_{q=1}^d \left[ 1 - \frac{\sum_{n=1}^N (\mathbf{a}_q^{(n)} - \hat{\mathbf{a}}_q^{(n)})^2}{\sum_{n=1}^N (\mathbf{a}_q^{(n)} - \bar{\mathbf{a}}_q)^2} \right],$$

where  $d$  is the activation dimensionality, and  $\bar{\mathbf{a}}_q$  is the mean activation for the  $q$ th dimension.

**Relative sparsity.** Since SAEs with different number of features are compared (e.g., across different ensemble sizes), we use a measure of sparsity relative to the total number of features:

$$\text{Relative Sparsity} = \frac{1}{N} \sum_{n=1}^N \frac{\left\| \mathbf{c}^{(n)} \right\|_0}{m}.$$

**Diversity.** This metric counts the number of dissimilar features in an SAE in terms of the maximum cosine similarity:

$$\text{Diversity} = \sum_{i=1}^m \mathbb{1} \left[ \max_{i \neq j} |\langle \mathbf{f}_i, \mathbf{f}_j \rangle| \leq \tau \right],$$

where  $\tau > 0$  is a threshold. Note that this metric does not depend on the evaluation tokens.

**Connectivity.** This metric, proposed in [15], measures the number of distinct pairs of SAE feature coefficients that are activated together across samples. It quantifies the diversity of the feature coefficients, with a high score indicating that a broad range of activations can be combined.

$$\text{Connectivity} = 1 - \left( \frac{1}{m^2} \left\| \mathbf{C}^\top \mathbf{C} \right\|_0 \right),$$

where  $\mathbf{C} \in \mathbb{R}^{N \times m}$  is the matrix of feature coefficients across all samples, and here  $\|\cdot\|_0$  counts the number of non-zero elements in a matrix.

**Stability.** This metric, adapted from [32], measures the maximum cosine similarity of the features that can be obtained across multiple runs of SAE training (with or without ensembling). Higher stability corresponds to the discovery of features that are similar across different runs. Note that this metric does not depend on the evaluation tokens. Given a total of  $S$  training runs, the stability for the  $s$ th run is:

$$\text{Stability} = \frac{1}{m} \sum_{i=1}^m \max_{s' \in [S] \setminus s, j \in [m]} \langle \mathbf{f}_i^{(s)}, \mathbf{f}_j^{(s')} \rangle.$$

### 5.1.3 Results

Figure 2 illustrates how the number of SAEs in the ensemble affects performance for both naive bagging and boosting on Gemma 2-2B. The first point in each plot represents a single SAE. Consistent

with prior work [27, 32],  $\tau = 0.7$  for the diversity metric. For completeness, we provide the results with additional values for  $\tau$  in Appendix E. Increasing the number of SAEs in the ensemble generally improves performance for most metrics and maintains the performance for the others. Comparing the two ensembling approaches, boosting outperforms naive bagging across all metrics except for stability. For example, boosting can explain more than 99% of the variance in the activations. Boosting also has a lower relative sparsity for  $>2$  SAEs in the ensemble, indicating that boosting requires fewer active features for the reconstructions. Further, the boosted SAE is also able to discover a higher number of diverse features, in terms of both feature directions and coefficients. Since boosting aims for bias reduction, it could learn more specific features, which can impact stability. Results for GELU-1L and Pythia-160M are provided in Appendix B, where a similar trend holds. Detailed results for ensembles of 8 SAEs across all three language models are summarized in Table 1. We ensemble up to 8 SAEs as most of the metrics start to plateau by then. Overall, we find that ensembling performs better than using a single SAE on the intrinsic metrics.

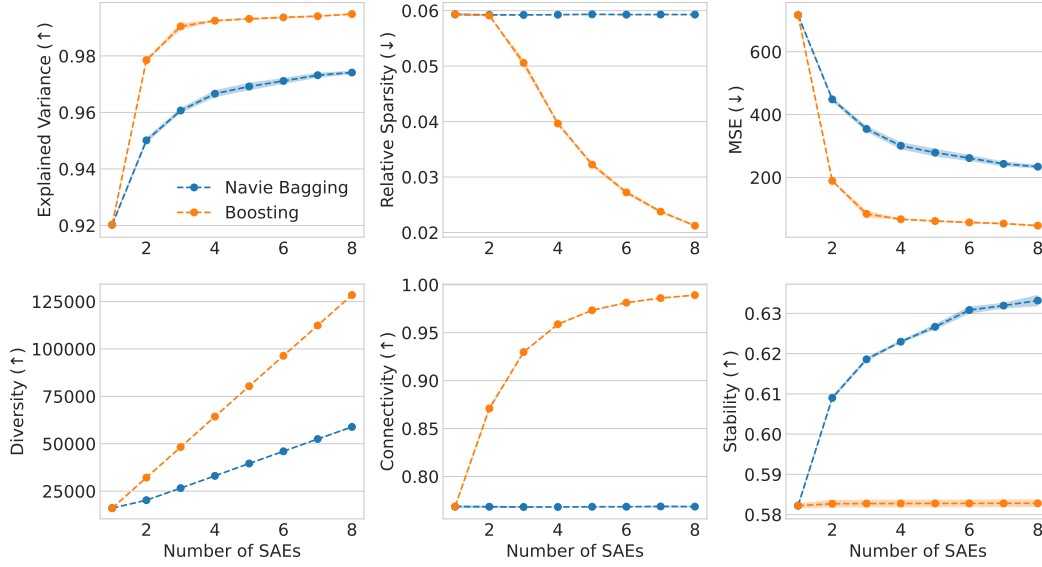


Figure 2: Effect of the number of SAEs in the ensemble for naive bagging and boosting on the intrinsic evaluation metrics for Gemma 2-2B. The shaded regions indicate 95% confidence intervals across 5 different experiment runs. For naive bagging, the different experiment runs correspond to different sets of initial weights.

Table 1: Intrinsic evaluation metrics for a single SAE, naive bagging, and boosting (ensembling 8 SAEs). Means along with 95% confidence intervals are reported across 5 experiment runs.

Ensembling Method	Explained Variance (↑)	Relative Sparsity (↓)	MSE (↓)	Diversity (↑)	Connectivity (↑)	Stability (↑)
<b>GELU-1L</b>						
Single SAE	0.875 (0.0020)	0.023 (0.0002)	41.694 (0.536)	16276.7 (10.47)	0.307 (0.0057)	0.705 (0.0016)
Naive Bagging	0.895 (0.0006)	0.023 (0.0000)	35.147 (0.210)	53087.0 (179.24)	0.307 (0.0009)	<b>0.745 (0.0002)</b>
Boosting	<b>0.961 (0.0018)</b>	<b>0.006 (0.0000)</b>	<b>12.542 (0.589)</b>	<b>130913.0 (5.48)</b>	<b>0.945 (0.0004)</b>	0.707 (0.0014)
<b>Pythia-160M</b>						
Single SAE	0.906 (0.0003)	0.008 (0.0000)	32.965 (0.077)	15804.5 (0.02)	0.912 (0.0013)	0.677 (0.0026)
Naive Bagging	0.929 (0.0000)	0.008 (0.0000)	24.704 (0.019)	50390.0 (0.05)	0.912 (0.0006)	<b>0.731 (0.0017)</b>
Boosting	<b>0.998 (0.0021)</b>	0.008 (0.0000)	<b>0.845 (0.547)</b>	<b>117018.2 (0.09)</b>	<b>0.986 (0.0004)</b>	0.680 (0.0025)
<b>Gemma 2-2B</b>						
Single SAE	0.920 (0.0006)	0.059 (0.0002)	716.659 (5.875)	16013.0 (5.88)	0.768 (0.0016)	0.581 (0.0006)
Naive Bagging	0.974 (0.0006)	0.059 (0.0000)	234.128 (6.228)	58859.6 (295.38)	0.769 (0.0007)	<b>0.633 (0.0014)</b>
Boosting	<b>0.995 (0.0003)</b>	<b>0.021 (0.0002)</b>	<b>46.538 (2.923)</b>	<b>128415.6 (114.89)</b>	<b>0.9891 (0.0003)</b>	0.583 (0.0009)

## 5.2 Use Case 1: Concept Detection

Interpretability use cases of SAEs such as debiasing and understanding sparse circuits often require individual SAE features to correspond to semantic concepts [8, 28]. Therefore, here we apply our ensemble approaches to detect semantic concepts across a range of domains. Specifically, per-token activations are encoded using an ensembled SAE, and mean-pooling is applied to obtain a sequence-level embedding. The SAE feature having the maximum mean difference between samples with and without the concept in the training set is selected to train a logistic regression classifier. Finally, accuracy on a held-out test set is used to evaluate the concept detection performance. We note that this evaluation procedure follows prior work [19, 23].

**Setup.** We train a ReLU SAE as the base SAE on the residual stream activations from layer 4 of Pythia-70M, with 100 million tokens from the Pile [18]. This setting is chosen since it has been used for concept-level tasks [22, 28]. Our concept detection use case encompasses four datasets and five tasks: **(1) Amazon Review (Category):** predicting product category from the reviews, **(2) Amazon Review (Sentiment):** predicting the sentiment of the review (1 vs. 5 stars), **(3) GitHub Code:** identifying the coding language from source code, **(4) AG News:** classifying news articles by topics, and **(5) European Parliament:** detecting the language of a document.

**Results.** Table 2 illustrates the results of the concept detection task for our ensemble approaches (with 8 SAEs in each ensemble). On average, ensembling approaches perform better than a single SAE across all the concept detection tasks. Comparing the two ensemble approaches, naive bagging generally performs better than boosting, although boosting still outperforms the single SAE for three out of the five datasets. One reason for the higher performance of naive bagging could be that it identifies features at a conceptual hierarchy which is suitable for this task. Also, boosting can potentially identify features that are too specific to the edge cases in the SAE training data rather than those that can be mapped to generalizable concepts. However, we note that if more than one feature is selected to train the logistic regression classifier, redundancy in features can potentially make detection performance stagnant for naive bagging (Appendix C).

Table 2: Test accuracy of the logistic regression classifier for the top concept-associated feature across five concept detection tasks for ensembles with 8 SAEs. Means along with 95% confidence intervals are reported across 5 experiment runs.

	Amazon Review (Category)	Amazon Review (Sentiment)	GitHub Code (Language)	AG News (Topic)	European Parliament (Language)
Single SAE	0.632 (0.033)	0.618 (0.030)	0.711 (0.020)	0.733 (0.021)	0.938 (0.016)
Naive Bagging	<b>0.665 (0.014)</b>	<b>0.631 (0.036)</b>	<b>0.715 (0.012)</b>	0.742 (0.037)	<b>0.943 (0.016)</b>
Boosting	0.655 (0.017)	0.624 (0.037)	0.682 (0.021)	<b>0.759 (0.021)</b>	0.920 (0.015)

## 5.3 Use Case 2: Spurious Correlation Removal

Neural networks have been previously shown to encode spurious correlations between non-essential input signals (e.g. image background) and the target label, which can negatively impact their generalization performance and robustness [10, 39]. Such biases can get exacerbated in more complex networks like large language models [25, 30]. Motivated by this, we consider the task of spurious correlation removal (SCR), as proposed in [22]. The evaluation procedure here follows [23] and is an automated version of Sparse Human-Interpretable Feature Trimming (SHIFT) [28].

**Setup.** The goal of SCR is to identify specific SAE features for the spurious signal and debias a classifier by ablating those features. Here we use the Bias in Bios dataset [9], which maps professional biographies to profession and gender. First, the dataset is filtered for a pair of professions (e.g. professor and nurse) and then it is partitioned into two sets: one which is balanced in terms of profession and gender, and the other with biased gender association for a particular profession (e.g. male professors and female nurses). Then, a linear classifier  $C_b$  is trained on the biased set using the activations from a language model. The goal is to debias this classifier to improve the accuracy on classifying profession in an unbiased held-out set.



To achieve that, a set of top  $L$  SAE features is identified based on their probe attribution scores for a probe trained to predict the spurious signal (i.e. gender) [23]. Then, a modified classifier  $C_m$  is trained after removing the spurious signal by zero-ablating the  $L$  SAE features. The predictive performance of the modified classifier  $C_m$  on profession for the held-out, balanced dataset indicates the SAE quality. Following [23], the normalized evaluation score  $S_{\text{SHIFT}}$  is defined as:

$$S_{\text{SHIFT}} = \frac{A_{\text{abl}} - A_{\text{base}}}{A_{\text{oracle}} - A_{\text{base}}},$$

where  $A_{\text{abl}}$  is the accuracy for  $C_m$ ,  $A_{\text{base}}$  is the accuracy for  $C_b$ , and  $A_{\text{oracle}}$  is the oracle accuracy with a classifier trained on a balanced dataset. It is worth noting that  $A_{\text{base}}$  and  $A_{\text{oracle}}$  do not depend on SAEs.

**Results.** The (ensembled) SAEs from Section 5.2 are used here, with  $L = 20$  features selected, following [23]. Table 3 shows the performance of our ensemble approaches for the SCR task across four pairs of profession, with the first profession biased towards males and the second towards females. Boosting consistently outperforms naive bagging and using a single SAE, across all pairs of professions, suggesting that it is more effective in isolating and removing gender-related features. Naive bagging does not perform as well as the single SAE, which could be because in naive bagging there are more than  $L$  similar features related to the spurious signal, and all of those features need to be ablated to observe an improved  $A_{\text{abl}}$ .

Table 3:  $S_{\text{SHIFT}}$  scores for the spurious correlation removal task with the top 20 gender-related features identified across four pairs of professions for ensembles with 8 SAEs. Means along with 95% confidence intervals are reported across 5 experiment runs.

	Professor vs. Nurse	Architect vs. Journalist	Surgeon vs. Psychologist	Attorney vs. Teacher
Single SAE	0.039 (0.008)	0.004 (0.006)	0.027 (0.006)	0.017 (0.003)
Naive Bagging	0.021 (0.003)	0.004 (0.001)	0.014 (0.002)	0.003 (0.005)
Boosting	<b>0.066 (0.016)</b>	<b>0.013 (0.011)</b>	<b>0.045 (0.014)</b>	<b>0.029 (0.003)</b>

## 6 Discussion

In this work, we propose ensembling SAEs as a way to improve performance by leveraging the feature variability of SAEs with the same architecture and hyperparameters. We instantiate two approaches, *naive bagging* and *boosting*. Theoretically, we justify both approaches as ways to improve reconstruction and show that ensembling in the output space of SAEs is equivalent to concatenation in the feature space. Empirically, we show that ensembling improves intrinsic performance, leading to better reconstruction of language model activations, more diverse features, and improved stability. We also demonstrate the practical utility of our ensembling approaches through quantitative validation on two downstream use cases, where ensembling can also outperform a single SAE.

Our ensemble approaches do come with some limitations. Both naive bagging and boosting are computationally more expensive than training a single SAE, since they require multiple SAEs to be trained. While this can be run in parallel for naive bagging, boosting has to be run sequentially. While ensembling performs better than a single SAE across all intrinsic metrics, this does not always translate to better downstream performance. For example, naive bagging could result in redundant features, causing a performance drop for tasks where multiple features are selected. On the other hand, boosting could learn features too specific to edge cases in the training set, leading to lower performance for detecting high-level, generalizable concepts. Thus, different ensemble approaches should be used based on the specific goals and procedures of downstream applications.

As a framework, SAE ensembling can be considered a meta-algorithm, which can be extended to different settings. We scope this work to focus on SAEs with the same architecture and hyperparameters, but future directions can consider ensembling (stacking) different architectures such as SAEs with different activation functions and sizes, stitched SAEs [26], and Matryoshka SAE [5]. Finally, future work can also explore ensembling from theoretical perspectives beyond reconstruction, such as feature identification.

## References

- [1] Charu C Aggarwal. Outlier ensembles: position paper. *ACM SIGKDD Explorations Newsletter*, 14(2):49–58, 2013.
- [2] Leo Breiman. Bagging predictors. *Machine learning*, 24:123–140, 1996.
- [3] Leo Breiman. Random forests. *Machine learning*, 45:5–32, 2001.
- [4] Trenton Bricken, Adly Templeton, Joshua Batson, Brian Chen, Adam Jermy, Tom Conerly, Nick Turner, Cem Anil, Carson Denison, Amanda Askell, Robert Lasenby, Yifan Wu, Shauna Kravec, Nicholas Schiefer, Tim Maxwell, Nicholas Joseph, Zac Hatfield-Dodds, Alex Tamkin, Karina Nguyen, Brayden McLean, Josiah E Burke, Tristan Hume, Shan Carter, Tom Henighan, and Christopher Olah. Towards monosemanticity: Decomposing language models with dictionary learning. *Transformer Circuits Thread*, 2023. <https://transformer-circuits.pub/2023/monosemantic-features/index.html>.
- [5] Bart Bussmann, Noa Nabeshima, Adam Karvonen, and Neel Nanda. Learning multi-level features with matryoshka sparse autoencoders. *arXiv preprint arXiv:2503.17547*, 2025.
- [6] David Chanin, James Wilken-Smith, Tomáš Dulka, Hardik Bhatnagar, and Joseph Bloom. A is for absorption: Studying feature splitting and absorption in sparse autoencoders. *arXiv preprint arXiv:2409.14507*, 2024.
- [7] Tianqi Chen and Carlos Guestrin. Xgboost: A scalable tree boosting system. In *Proceedings of the 22nd acm sigkdd international conference on knowledge discovery and data mining*, pages 785–794, 2016.
- [8] Hoagy Cunningham, Aidan Ewart, Logan Riggs, Robert Huben, and Lee Sharkey. Sparse autoencoders find highly interpretable features in language models. *arXiv preprint arXiv:2309.08600*, 2023.
- [9] Maria De-Arteaga, Alexey Romanov, Hanna Wallach, Jennifer Chayes, Christian Borgs, Alexandra Chouldechova, Sahin Geyik, Krishnaram Kenthapadi, and Adam Tauman Kalai. Bias in bios: A case study of semantic representation bias in a high-stakes setting. In *proceedings of the Conference on Fairness, Accountability, and Transparency*, pages 120–128, 2019.
- [10] Alex J DeGrave, Joseph D Janizek, and Su-In Lee. Ai for radiographic covid-19 detection selects shortcuts over signal. *Nature Machine Intelligence*, 3(7):610–619, 2021.
- [11] Carlotta Domeniconi and Muna Al-Razgan. Weighted cluster ensembles: Methods and analysis. *ACM Transactions on Knowledge Discovery from Data (TKDD)*, 2(4):1–40, 2009.
- [12] Nasrollah Etemadi. An elementary proof of the strong law of large numbers. *Zeitschrift für Wahrscheinlichkeitstheorie und verwandte Gebiete*, 55(1):119–122, 1981.
- [13] Eoin Farrell, Yeu-Tong Lau, and Arthur Conmy. Applying sparse autoencoders to unlearn knowledge in language models. *arXiv preprint arXiv:2410.19278*, 2024.
- [14] Thomas Fel, Victor Boutin, Louis Béthune, Rémi Cadène, Mazda Moayeri, Léo Andéol, Mathieu Chalvidal, and Thomas Serre. A holistic approach to unifying automatic concept extraction and concept importance estimation. *Advances in Neural Information Processing Systems*, 36:54805–54818, 2023.
- [15] Thomas Fel, Ekdeep Singh Lubana, Jacob S Prince, Matthew Kowal, Victor Boutin, Isabel Papadimitriou, Binxu Wang, Martin Wattenberg, Demba Ba, and Talia Konkle. Archetypal sae: Adaptive and stable dictionary learning for concept extraction in large vision models. *arXiv preprint arXiv:2502.12892*, 2025.
- [16] Xiaoli Zhang Fern and Carla E Brodley. Solving cluster ensemble problems by bipartite graph partitioning. In *Proceedings of the twenty-first international conference on Machine learning*, page 36, 2004.
- [17] Jerome H Friedman. Greedy function approximation: a gradient boosting machine. *Annals of statistics*, pages 1189–1232, 2001.

- [18] Leo Gao, Stella Biderman, Sid Black, Laurence Golding, Travis Hoppe, Charles Foster, Jason Phang, Horace He, Anish Thite, Noa Nabeshima, et al. The pile: An 800gb dataset of diverse text for language modeling. *arXiv preprint arXiv:2101.00027*, 2020.
- [19] Leo Gao, Tom Dupré la Tour, Henk Tillman, Gabriel Goh, Rajan Troll, Alec Radford, Ilya Sutskever, Jan Leike, and Jeffrey Wu. Scaling and evaluating sparse autoencoders. *arXiv preprint arXiv:2406.04093*, 2024.
- [20] Joydeep Ghosh and Ayan Acharya. Cluster ensembles. *Wiley interdisciplinary reviews: Data mining and knowledge discovery*, 1(4):305–315, 2011.
- [21] Sai Sumedh R Hindupur, Ekdeep Singh Lubana, Thomas Fel, and Demba Ba. Projecting assumptions: The duality between sparse autoencoders and concept geometry. *arXiv preprint arXiv:2503.01822*, 2025.
- [22] Adam Karvonen, Can Rager, Samuel Marks, and Neel Nanda. Evaluating sparse autoencoders on targeted concept erasure tasks. *arXiv preprint arXiv:2411.18895*, 2024.
- [23] Adam Karvonen, Can Rager, Johnny Lin, Curt Tigges, Joseph Bloom, David Chanin, Yeu-Tong Lau, Eoin Farrell, Callum McDougall, Kola Ayonrinde, et al. Saebench: A comprehensive benchmark for sparse autoencoders in language model interpretability. *arXiv preprint arXiv:2503.09532*, 2025.
- [24] Diederik P Kingma and Jimmy Ba. Adam: A method for stochastic optimization. *arXiv preprint arXiv:1412.6980*, 2014.
- [25] Hadas Kotek, Rikker Dockum, and David Sun. Gender bias and stereotypes in large language models. In *Proceedings of the ACM collective intelligence conference*, pages 12–24, 2023.
- [26] Patrick Leask, Bart Bussmann, Michael Pearce, Joseph Bloom, Curt Tigges, Noura Al Moubayed, Lee Sharkey, and Neel Nanda. Sparse autoencoders do not find canonical units of analysis. *arXiv preprint arXiv:2502.04878*, 2025.
- [27] Tom Lieberum, Senthooan Rajamanoharan, Arthur Conmy, Lewis Smith, Nicolas Sonnerat, Vikrant Varma, János Kramár, Anca Dragan, Rohin Shah, and Neel Nanda. Gemma scope: Open sparse autoencoders everywhere all at once on gemma 2. *arXiv preprint arXiv:2408.05147*, 2024.
- [28] Samuel Marks, Can Rager, Eric J Michaud, Yonatan Belinkov, David Bau, and Aaron Mueller. Sparse feature circuits: Discovering and editing interpretable causal graphs in language models. *arXiv preprint arXiv:2403.19647*, 2024.
- [29] Rajiv Movva, Kenny Peng, Nikhil Garg, Jon Kleinberg, and Emma Pierson. Sparse autoencoders for hypothesis generation. *arXiv preprint arXiv:2502.04382*, 2025.
- [30] Roberto Navigli, Simone Conia, and Björn Ross. Biases in large language models: origins, inventory, and discussion. *ACM Journal of Data and Information Quality*, 15(2):1–21, 2023.
- [31] Kyle O’Brien, David Majercak, Xavier Fernandes, Richard Edgar, Jingya Chen, Harsha Nori, Dean Carignan, Eric Horvitz, and Forough Poursabzi-Sangde. Steering language model refusal with sparse autoencoders. *arXiv preprint arXiv:2411.11296*, 2024.
- [32] Gonçalo Paulo and Nora Belrose. Sparse autoencoders trained on the same data learn different features. *arXiv preprint arXiv:2501.16615*, 2025.
- [33] Senthooan Rajamanoharan, Arthur Conmy, Lewis Smith, Tom Lieberum, Vikrant Varma, János Kramár, Rohin Shah, and Neel Nanda. Improving dictionary learning with gated sparse autoencoders. *arXiv preprint arXiv:2404.16014*, 2024.
- [34] Senthooan Rajamanoharan, Tom Lieberum, Nicolas Sonnerat, Arthur Conmy, Vikrant Varma, János Kramár, and Neel Nanda. Jumping ahead: Improving reconstruction fidelity with jumprelu sparse autoencoders. *arXiv preprint arXiv:2407.14435*, 2024.

- [35] Sukrut Rao, Sweta Mahajan, Moritz Böhle, and Bernt Schiele. Discover-then-name: Task-agnostic concept bottlenecks via automated concept discovery. In *European Conference on Computer Vision*, pages 444–461. Springer, 2024.
- [36] David H Wolpert. Stacked generalization. *Neural networks*, 5(2):241–259, 1992.
- [37] Mitchell Wortsman, Gabriel Ilharco, Samir Ya Gadre, Rebecca Roelofs, Raphael Gontijo-Lopes, Ari S Morcos, Hongseok Namkoong, Ali Farhadi, Yair Carmon, Simon Kornblith, et al. Model soups: averaging weights of multiple fine-tuned models improves accuracy without increasing inference time. In *International conference on machine learning*, pages 23965–23998. PMLR, 2022.
- [38] Mitchell Wortsman, Gabriel Ilharco, Jong Wook Kim, Mike Li, Simon Kornblith, Rebecca Roelofs, Raphael Gontijo Lopes, Hannaneh Hajishirzi, Ali Farhadi, Hongseok Namkoong, et al. Robust fine-tuning of zero-shot models. In *Proceedings of the IEEE/CVF conference on computer vision and pattern recognition*, pages 7959–7971, 2022.
- [39] Wenqian Ye, Guangtao Zheng, Xu Cao, Yunsheng Ma, and Aidong Zhang. Spurious correlations in machine learning: A survey. *arXiv preprint arXiv:2402.12715*, 2024.
- [40] Arthur Zimek, Ricardo JGB Campello, and Jörg Sander. Ensembles for unsupervised outlier detection: challenges and research questions a position paper. *Acm Sigkdd Explorations Newsletter*, 15(1):11–22, 2014.

## A Theoretical Results

Here we (re-)state and prove our results from Section 3.2, Section 4.1, and Section 4.2.

**Proposition 1.** *Suppose there are  $J$  SAEs  $g(\cdot; \theta^{(1)}), \dots, g(\cdot; \theta^{(J)})$ , with decoder matrices  $\mathbf{W}_{dec}^{(1)}, \dots, \mathbf{W}_{dec}^{(J)} \in \mathbb{R}^{d \times k}$  and decoder biases  $\mathbf{b}_{dec}^{(1)}, \dots, \mathbf{b}_{dec}^{(J)} \in \mathbb{R}^d$ . For a given neural network activation  $\mathbf{a} \in \mathbb{R}^d$ , let  $\mathbf{c}^{(1)}, \dots, \mathbf{c}^{(J)} \in \mathbb{R}^k$  denote the feature coefficients. Then ensembling the  $J$  SAEs is equivalent to reconstructing  $\mathbf{a}$  with:*

$$\hat{\mathbf{a}} = \mathbf{W}_{dec} \mathbf{c} + \mathbf{b}_{dec} = \sum_{i'=1}^{kJ} \mathbf{c}_{i'} \mathbf{f}_{i'} + \mathbf{b}_{dec}, \quad (10)$$

where

$$\mathbf{c} = \begin{bmatrix} \alpha^{(1)} \mathbf{c}^{(1)} \\ \vdots \\ \alpha^{(J)} \mathbf{c}^{(J)} \end{bmatrix}, \mathbf{W}_{dec} = [\mathbf{W}_{dec}^{(1)} \dots \mathbf{W}_{dec}^{(J)}], \mathbf{b}_{dec} = \sum_{j=1}^J \alpha^{(j)} \mathbf{b}_{dec}^{(j)}, \quad (11)$$

and  $\mathbf{f}_{i'} = \mathbf{W}_{dec}[:, i']$ , with  $\mathbf{c} \in \mathbb{R}^{kJ}$ ,  $\mathbf{W}_{dec} \in \mathbb{R}^{d \times kJ}$ ,  $\mathbf{b}_{dec} \in \mathbb{R}^d$ .

*Proof.* Based on the definition of an SAE ensemble in Equation (4) and the definition of feature coefficients, we have

$$\hat{\mathbf{a}} = \sum_{j=1}^J \alpha^{(j)} \left( \mathbf{W}_{dec}^{(j)} \mathbf{c}^{(j)} + \mathbf{b}_{dec}^{(j)} \right) \quad (12)$$

$$= [\mathbf{W}_{dec}^{(1)} \dots \mathbf{W}_{dec}^{(J)}] \begin{bmatrix} \alpha^{(1)} \mathbf{c}^{(1)} \\ \vdots \\ \alpha^{(J)} \mathbf{c}^{(J)} \end{bmatrix} + \sum_{j=1}^J \alpha^{(j)} \mathbf{b}_{dec}^{(j)} \quad (13)$$

$$= \mathbf{W}_{dec} \mathbf{c} + \mathbf{b}_{dec}, \quad (14)$$

where Equation (13) follows from observing that the sum of matrix-vector product is equivalent to the product of the concatenated matrix and vector.  $\square$

Here, we provide a lemma showing the bias-variance decomposition for reconstructing a neural network activation with an ensembled SAE (Section 3.2).

**Lemma 1.** *Given a neural network activation  $\mathbf{a}^{(*)}$ , and the ensembled SAE  $g_{Ens}(\cdot; \{\theta^{(j)}\}_{j=1}^J)$  trained on activations  $\{\mathbf{a}^{(n)}\}_{n=1}^N$ , the expected reconstruction error can be decomposed into a bias term and a variance term. That is,*

$$\mathbb{E}_{\{\theta^{(j)}\}_{j=1}^J | \{\mathbf{a}^{(n)}\}_{n=1}^N} \left[ \left\| \mathbf{a}^{(*)} - g_{Ens}(\mathbf{a}^{(*)}; \{\theta^{(j)}\}_{j=1}^J) \right\|_2^2 \right] \quad (15)$$

$$= \underbrace{\left\| \mathbf{a}^{(*)} - \mathbb{E}_{\{\theta^{(j)}\}_{j=1}^J | \{\mathbf{a}^{(n)}\}_{n=1}^N} [g_{Ens}(\mathbf{a}^{(*)}; \{\theta^{(j)}\}_{j=1}^J)] \right\|_2^2}_{\text{bias term}} \quad (16)$$

$$+ \underbrace{\mathbb{E}_{\{\theta^{(j)}\}_{j=1}^J | \{\mathbf{a}^{(n)}\}_{n=1}^N} \left[ \left\| \mathbb{E}_{\{\theta^{(j)}\}_{j=1}^J | \{\mathbf{a}^{(n)}\}_{n=1}^N} [g_{Ens}(\mathbf{a}^{(*)}; \{\theta^{(j)}\}_{j=1}^J)] - g_{Ens}(\mathbf{a}^{(*)}; \{\theta^{(j)}\}_{j=1}^J) \right\|_2^2 \right]}_{\text{variance term}}. \quad (17)$$

*Proof.* Since all the expectations are taken with respect to the same randomness, their subscripts are dropped for notational ease. Also, let  $\Theta^{(J)} = \{\theta^{(j)}\}_{j=1}^J$ . We have

$$\mathbb{E} \left[ \left\| \mathbf{a}^{(*)} - g_{\text{Ens}}(\mathbf{a}^{(*)}; \Theta^{(J)}) \right\|_2^2 \right] \quad (18)$$

$$= \mathbb{E} \left[ \left\| \mathbf{a}^{(*)} - \mathbb{E}[g_{\text{Ens}}(\mathbf{a}^{(*)}; \Theta^{(J)})] + \mathbb{E}[g_{\text{Ens}}(\mathbf{a}^{(*)}; \Theta^{(J)})] - g_{\text{Ens}}(\mathbf{a}^{(*)}; \Theta^{(J)}) \right\|_2^2 \right] \quad (19)$$

$$= \mathbb{E} \left[ \left\| \mathbf{a}^{(*)} - \mathbb{E}[g_{\text{Ens}}(\mathbf{a}^{(*)}; \Theta^{(J)})] \right\|_2^2 \right] \quad (20)$$

$$+ \mathbb{E} \left[ \left\| \mathbb{E}[g_{\text{Ens}}(\mathbf{a}^{(*)}; \Theta^{(J)})] - g_{\text{Ens}}(\mathbf{a}^{(*)}; \Theta^{(J)}) \right\|_2^2 \right] \quad (21)$$

$$+ 2\mathbb{E} \left[ \left( \mathbf{a}^{(*)} - \mathbb{E}[g_{\text{Ens}}(\mathbf{a}^{(*)}; \Theta^{(J)})] \right)^\top \left( \mathbb{E}[g_{\text{Ens}}(\mathbf{a}^{(*)}; \Theta^{(J)})] - g_{\text{Ens}}(\mathbf{a}^{(*)}; \Theta^{(J)}) \right) \right]. \quad (22)$$

Because  $\mathbf{a}^{(*)}$  and  $\mathbb{E}[g_{\text{Ens}}(\mathbf{a}^{(*)}; \Theta^{(J)})]$  are constants with respect to the expectation, for (20) we have

$$\mathbb{E} \left[ \left\| \mathbf{a}^{(*)} - \mathbb{E}[g_{\text{Ens}}(\mathbf{a}^{(*)}; \Theta^{(J)})] \right\|_2^2 \right] = \left\| \mathbf{a}^{(*)} - \mathbb{E}[g_{\text{Ens}}(\mathbf{a}^{(*)}; \Theta^{(J)})] \right\|_2^2, \quad (23)$$

which is the stated bias term.

For the last term in (22), we have

$$\mathbb{E} \left[ \left( \mathbf{a}^{(*)} - \mathbb{E}[g_{\text{Ens}}(\mathbf{a}^{(*)}; \Theta^{(J)})] \right)^\top \left( \mathbb{E}[g_{\text{Ens}}(\mathbf{a}^{(*)}; \Theta^{(J)})] - g_{\text{Ens}}(\mathbf{a}^{(*)}; \Theta^{(J)}) \right) \right] \quad (24)$$

$$= \left( \mathbf{a}^{(*)} - \mathbb{E}[g_{\text{Ens}}(\mathbf{a}^{(*)}; \Theta^{(J)})] \right)^\top \left( \mathbb{E}[g_{\text{Ens}}(\mathbf{a}^{(*)}; \Theta^{(J)})] - \mathbb{E}[g_{\text{Ens}}(\mathbf{a}^{(*)}; \Theta^{(J)})] \right) = 0, \quad (25)$$

again because  $\mathbf{a}^{(*)}$  and  $\mathbb{E}[g_{\text{Ens}}(\mathbf{a}^{(*)}; \Theta^{(J)})]$  are constants with respect to the expectation. Taken together, we have

$$\mathbb{E} \left[ \left\| \mathbf{a}^{(*)} - g_{\text{Ens}}(\mathbf{a}^{(*)}; \Theta^{(J)}) \right\|_2^2 \right] \quad (26)$$

$$= \left\| \mathbf{a}^{(*)} - \mathbb{E}[g_{\text{Ens}}(\mathbf{a}^{(*)}; \Theta^{(J)})] \right\|_2^2 + \mathbb{E} \left[ \left\| \mathbb{E}[g_{\text{Ens}}(\mathbf{a}^{(*)}; \Theta^{(J)})] - g_{\text{Ens}}(\mathbf{a}^{(*)}; \Theta^{(J)}) \right\|_2^2 \right], \quad (27)$$

where the first term is the stated bias term, and the second term is the stated variance term.  $\square$

We now show that naive bagging (Section 4.1) can reduce the reconstruction variance above. Formally, we have the following proposition.

**Proposition 2.** *Given a neural network activation  $\mathbf{a}^{(*)}$  and the ensembled SAE  $g_{\text{NB}}(\cdot; \{\theta^{(j)}\}_{j=1}^J)$  obtained through naive bagging trained on activations  $\{\mathbf{a}^{(n)}\}_{n=1}^N$ , the variance term in Lemma 1 goes to zero almost surely as  $J \rightarrow \infty$ .*

*Proof.* For notational ease, let  $\mathbf{A} = \{\mathbf{a}^{(n)}\}_{n=1}^N$ , and  $\Theta^{(J)} = \{\theta^{(j)}\}_{j=1}^J$ . By the definition of naive bagging, we have

$$g_{\text{NB}}(\mathbf{a}^{(*)}; \Theta^{(J)}) = \frac{1}{J} \sum_{j=1}^J g(\mathbf{a}^{(*)}; \theta^{(j)}). \quad (28)$$

It follows that the variance term in Lemma 1 can be written as

$$\mathbb{E}_{\Theta^{(J)}|\mathbf{A}} \left[ \left\| \mathbb{E}_{\Theta^{(J)}|\mathbf{A}} \left[ \frac{1}{J} \sum_{j=1}^J g(\mathbf{a}^{(*)}; \theta^{(j)}) \right] - \frac{1}{J} \sum_{j=1}^J g(\mathbf{a}^{(*)}; \theta^{(j)}) \right\|_2^2 \right] \quad (29)$$

$$= \mathbb{E}_{\Theta^{(J)}|\mathbf{A}} \left[ \left\| \mathbb{E}_{\theta|\mathbf{A}}[g(\mathbf{a}^{(*)}; \theta)] - \frac{1}{J} \sum_{j=1}^J g(\mathbf{a}^{(*)}; \theta^{(j)}) \right\|_2^2 \right], \quad (30)$$

where (30) follows from the linearity of expectation, and from the fact that  $\theta^{(1)}, \dots, \theta^{(J)}$  are identically distributed when conditioned on  $\mathbf{A}$ .

For practical neural networks and SAEs, we can assume that

$$\mathbb{E}_{\theta|\mathbf{A}} [g_q(\mathbf{a}^{(*)}; \theta)] < \infty, \quad (31)$$

for each dimension  $q \in [d]$ . Furthermore, conditioned on  $\mathbf{A}$ , the trainings of  $\theta^{(1)}, \dots, \theta^{(J)}$  are identically and independently distributed. Therefore, we can apply the strong law of large numbers [12], obtaining

$$\frac{1}{J} \sum_{j=1}^J g_q(\mathbf{a}^{(*)}; \theta^{(j)}) = \mathbb{E}_{\theta|\mathbf{A}} [g_q(\mathbf{a}^{(*)}; \theta)] \quad (32)$$

almost surely as  $J \rightarrow \infty$ . It then follows that

$$\frac{1}{J} \sum_{j=1}^J g(\mathbf{a}^{(*)}; \theta^{(j)}) = \mathbb{E}_{\theta|\mathbf{A}} [g(\mathbf{a}^{(*)}; \theta)], \quad (33)$$

and for the variance term in Lemma 1:

$$\mathbb{E}_{\Theta^{(J)}|\mathbf{A}} \left[ \left\| \mathbb{E}_{\theta|\mathbf{A}} [g(\mathbf{a}^{(*)}; \theta)] - \frac{1}{J} \sum_{j=1}^J g(\mathbf{a}^{(*)}; \theta^{(j)}) \right\|_2^2 \right] \quad (34)$$

$$= \mathbb{E}_{\Theta^{(J)}|\mathbf{A}} \left[ \left\| \mathbb{E}_{\theta|\mathbf{A}} [g(\mathbf{a}^{(*)}; \theta)] - \mathbb{E}_{\theta|\mathbf{A}} [g(\mathbf{a}^{(*)}; \theta)] \right\|_2^2 \right] = 0, \quad (35)$$

almost surely as  $J \rightarrow \infty$ .  $\square$

**Remark 2.** We note that all the expectations in the bias-variance decomposition in Lemma 1 are conditioned on the specific training set  $\{\mathbf{a}^{(n)}\}_{n=1}^N$ . This conditioning is needed for Proposition 2 to hold. Otherwise separate training runs of the SAE are dependent through the training set.

We now discuss the two assumptions needed for bounding the bias term in Lemma 1 for boosting (Section 4.2).

**Assumption 1.** For a given neural network activation  $\mathbf{a}^{(*)}$  and the ensembled SAE  $g_{\text{Boost}}(\cdot; \{\theta^{(j)}\}_{j=1}^J)$  obtained through boosting trained on the activations  $\{\mathbf{a}^{(n)}\}_{n=1}^N$ , we assume that

$$\left\| \mathbf{a}^{(*)} - \mathbb{E}_{\{\theta^{(j)}\}_{j=1}^J | \{\mathbf{a}^{(n)}\}_{n=1}^N} [g_{\text{Boost}}(\mathbf{a}^{(*)}; \{\theta^{(j)}\}_{j=1}^J)] \right\|_2^2 \quad (36)$$

$$\leq \frac{1}{N} \sum_{n=1}^N \left\| \mathbf{a}^{(n)} - \mathbb{E}_{\{\theta^{(j)}\}_{j=1}^J | \{\mathbf{a}^{(n)}\}_{n=1}^N} [g_{\text{Boost}}(\mathbf{a}^{(n)}; \{\theta^{(j)}\}_{j=1}^J)] \right\|_2^2 + \varepsilon_G, \quad (37)$$

for some constant  $\varepsilon_G > 0$ .

**Remark 3.** Assumption 1 is essentially a generalization bound on the reconstruction performance for boosting. Intuitively, this assumption can hold because SAEs are regularized. However, note that this assumption can break down when  $\mathbf{a}^{(*)}$  is much different from  $\{\mathbf{a}^{(n)}\}_{n=1}^N$ , which is a general pitfall for generalization bounds.

**Assumption 2.** For the ensembled SAE  $g_{\text{Boost}}(\cdot; \{\theta^{(j)}\}_{j=1}^J)$  obtained through boosting trained on the activations  $\{\mathbf{a}^{(n)}\}_{n=1}^N$ , we assume that as  $J \rightarrow \infty$ ,

$$\frac{1}{N} \sum_{n=1}^N \left\| \mathbf{a}^{(n)} - \mathbb{E}_{\{\theta^{(j)}\}_{j=1}^J | \{\mathbf{a}^{(n)}\}_{n=1}^N} [g_{\text{Boost}}(\mathbf{a}^{(n)}; \{\theta^{(j)}\}_{j=1}^J)] \right\|_2^2 \leq \varepsilon_I, \quad (38)$$

for some constant  $\varepsilon_I > 0$ .

**Remark 4.** Assumption 2 formalizes the intuition that boosting should be able to overfit almost perfectly to the training set. However, there is some irreducible error  $\varepsilon_I$  because SAEs are simple and regularized models. This intuition is empirically verified in Supplementary Figure 1.

We now present the proposition showing that boosting with more iterations can lead to a bounded bias term in Lemma 1.

**Proposition 3.** *For a given neural network activation  $\mathbf{a}^{(*)}$  and the ensembled SAE  $g_{\text{Boost}}(\cdot; \{\theta^{(j)}\}_{j=1}^J)$  obtained through boosting trained on the activations  $\{\mathbf{a}^{(n)}\}_{n=1}^N$ , under Assumption 1 and Assumption 2 we have, as  $J \rightarrow \infty$ ,*

$$\left\| \mathbf{a}^{(*)} - \mathbb{E}_{\{\theta^{(j)}\}_{j=1}^J | \{\mathbf{a}^{(n)}\}_{n=1}^N} [g_{\text{Boost}}(\mathbf{a}^{(*)}; \{\theta^{(j)}\}_{j=1}^J)] \right\|_2^2 \leq \varepsilon, \quad (39)$$

for some constant  $\varepsilon > 0$ .

*Proof.* The proof follows immediately under the assumptions. We have

$$\left\| \mathbf{a}^{(*)} - \mathbb{E}_{\{\theta^{(j)}\}_{j=1}^J | \{\mathbf{a}^{(n)}\}_{n=1}^N} [g_{\text{Boost}}(\mathbf{a}^{(*)}; \{\theta^{(j)}\}_{j=1}^J)] \right\|_2^2 \quad (40)$$

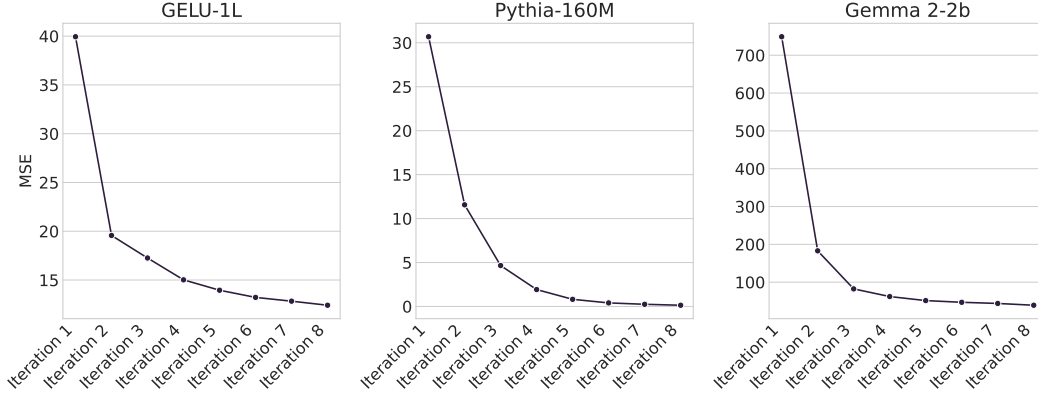
$$\leq \frac{1}{N} \sum_{n=1}^N \left\| \mathbf{a}^{(n)} - \mathbb{E}_{\{\theta^{(j)}\}_{j=1}^J | \{\mathbf{a}^{(n)}\}_{n=1}^N} [g_{\text{Boost}}(\mathbf{a}^{(n)}; \{\theta^{(j)}\}_{j=1}^J)] \right\|_2^2 + \varepsilon_G \quad (41)$$

$$\leq \varepsilon_I + \varepsilon_G, \quad (42)$$

where (41) uses Assumption 1, and (42) uses Assumption 2. Setting  $\varepsilon = \varepsilon_I + \varepsilon_G$  completes the proof.  $\square$

**Remark 5.** Proposition 3 is not surprising given Assumption 1 and Assumption 2. However, this formalization gives us insights about reasons why boosting may fail to reduce the bias term in the generalization region. That is, Assumption 1 or Assumption 2 may not hold (e.g. due to distribution shift or having too many constraints on the SAE, respectively).

**Remark 6.** Finally, we note that Proposition 2 and Proposition 3 are both asymptotic results with respect to the number of SAEs in the ensemble, primarily serving to motivate naive bagging and boosting from the perspective of the reconstruction error. Future work that relates reconstruction to the identifiability of human-interpretable features would be more directly useful for downstream interpretability tasks.

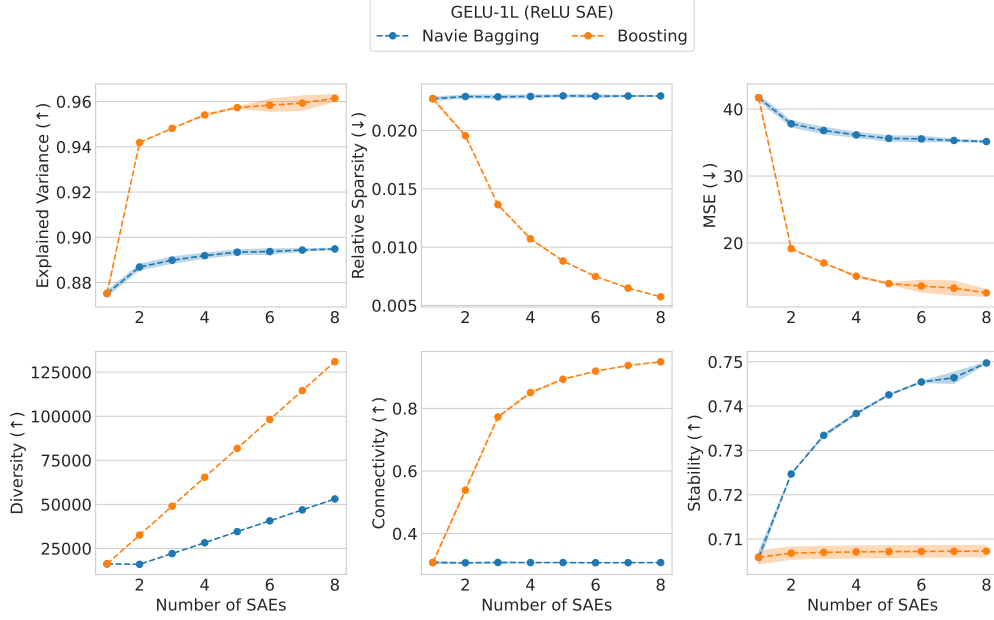


Supplementary Figure 1: MSE loss at the last training step for each iteration of a boosting ensemble with 8 SAEs. Reconstruction performance improves with each boosting iteration.

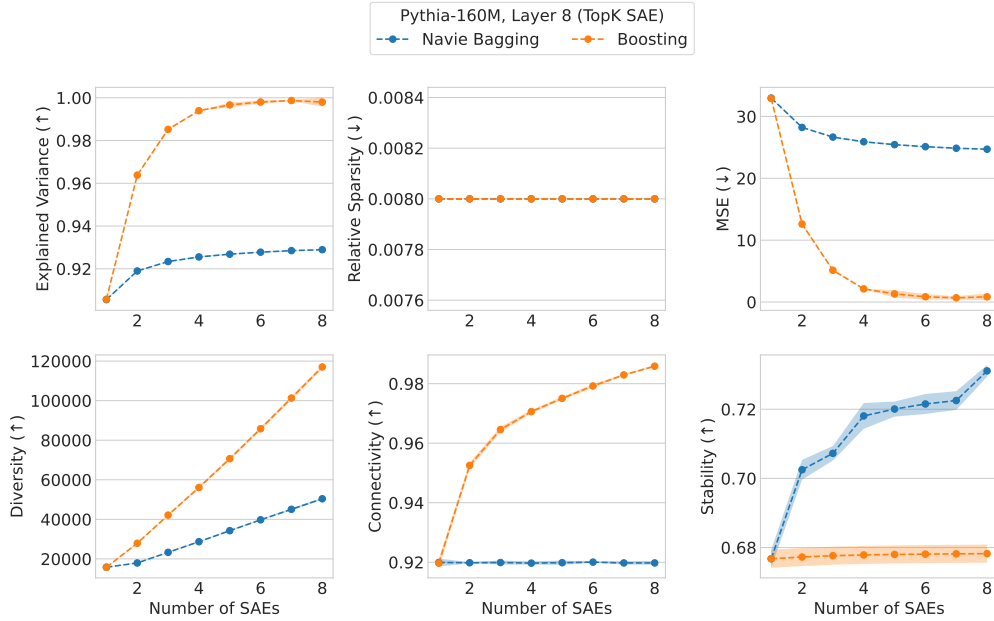


## B Results for GELU-1L and Pythia-160M

Here we show the results for the intrinsic evaluations of GELU-1L (Supplementary Figure 2) and Pythia-160M (Supplementary Figure 3), with  $\tau = 0.7$  for the diversity metric. Overall, the trend is similar to that of Gemma 2-2B. Performance on most of the metrics improves as more SAEs are added to the ensemble, although it saturates for some of them around 8 SAEs. Also, boosting outperforms naive bagging in all metrics except for stability.



Supplementary Figure 2: Intrinsic evaluation of the ensembling approaches for GELU-1L. The shaded regions indicate 95% confidence intervals across 5 experiment runs.



Supplementary Figure 3: Intrinsic evaluation of the ensembling approaches for Pythia-160M. The shaded regions indicate 95% confidence intervals across 5 experiment runs.

## C Additional Results for Downstream Use Cases

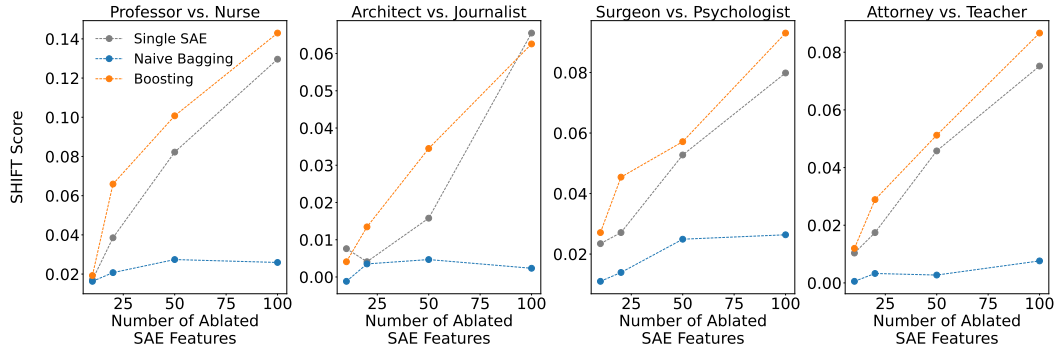
Here we provide additional results for the downstream use cases (Section 5.2 and Section 5.3).

Supplementary Table 1 shows the test accuracy of a classifier trained using the top-5 concept-associated features identified by the ensembling methods across five tasks. The results are slightly different from those in Section 5.2, with boosting outperforming naive bagging and the single SAE for four out of the five tasks. This suggests that, while boosting does not identify the top feature, additional features from boosting can be selected to improve concept detection.

Supplementary Table 1: Test accuracy of the logistic regression classifier for the top-5 concept-associated feature across five concept detection tasks. SAE Ensembles consist of 8 SAEs. Means along with 95% confidence intervals are reported across 5 experiment runs.

	Amazon Review (Category)	Amazon Review (Sentiment)	GitHub Code (Language)	AG News (Topic)	European Parliament (Language)
Single SAE	0.719 (0.011)	0.702 (0.015)	<b>0.805 (0.004)</b>	0.851 (0.005)	0.981 (0.003)
Naive Bagging	0.692 (0.010)	0.689 (0.015)	0.728 (0.005)	0.783 (0.023)	0.952 (0.004)
Boosting	<b>0.726 (0.008)</b>	<b>0.708 (0.016)</b>	0.795 (0.016)	<b>0.863 (0.008)</b>	<b>0.988 (0.000)</b>

Supplementary Figure 4 shows the  $S_{\text{SHIFT}}$  scores for the spurious correlation removal task as the number of top gender-related features is varied. The trend is similar to what is observed in Section 5.3, with boosting outperforming naive bagging and the single SAE for different numbers of ablated gender-related SAE features. The performance generally increases as the number of ablated features increases, indicating that there are multiple gender related features which are correctly identified by all the methods. This is especially worth noting for naive bagging, as increasing the number of ablated features might lead to all the redundant features related to the spurious signal getting ablated.



Supplementary Figure 4:  $S_{\text{SHIFT}}$  scores for the spurious correlation removal task vs. various numbers of top gender-related features identified across four pairs of professions. SAE ensembles consist of 8 SAEs. Means across 5 experiment runs are shown.

## D Implementation Details

Here we provide additional details about the data, compute, and hyperparameter selection.

### D.1 Dataset and Models

The Pile dataset [18] (with copyrighted contents removed) used for training the SAEs is a large, diverse, and open-source English text dataset curated specifically for training general-purpose language models. Its diverse components include academic papers (e.g., arXiv, PubMed Central), books (e.g., Books3, BookCorpus2), code (from GitHub), web content (e.g., a filtered version of Common Crawl called Pile-CC, OpenWebText2), and other sources like Wikipedia, Stack Exchange, and subtitles.

Beyond training, the Pile also serves as a benchmark for evaluating language models. More recently, the Pile has become the standard dataset for training sparse autoencoders [5, 8, 27, 28, 32].

All the language models we use have been previously used for training and evaluating sparse autoencoders [4, 19, 27, 32]. Supplementary Table 2 provides additional details on the language models and the corresponding SAE architectures.

Supplementary Table 2: Overview of the language models and SAE architectures used for intrinsic evaluation and downstream use cases.

Language Model	Num. Params	Num. Layers	Context Size	Activation Dimension	Layer Used	SAE Arch.
<b>Intrinsic Evaluation</b>						
GELU-1L	3.1M	1	1024	512	1	ReLU [8]
Pythia-160M	162.3M	12	2048	768	8	TopK [19]
Gemma 2-2B	2.1B	26	8192	2304	12	JumpReLU [34]
<b>Downstream Use Cases</b>						
Pythia-70M	70.4M	6	2048	512	4	ReLU

## D.2 Training

Our ensembling algorithms are implemented in PyTorch<sup>5</sup> by adapting the SAELens library.<sup>6</sup> The pseudocode for boosting is summarized in Algorithm 1. For naive bagging, the training procedure for each SAE in the ensemble is the same as the standard SAE training. All the SAEs and the ensembles are trained on either an A100 GPU with 80GB of memory or an H100 NVL GPU with 93 GB of memory using a batch size of 10000. Supplementary Table 3 shows the time taken for a single experiment run on a single H100 GPU for ensembles with 8 SAEs. It is worth noting that naive bagging can be parallelized across multiple GPUs, bringing down the training time to that of a single SAE when the number of GPUs is equal to the number of SAEs in the ensemble.

Supplementary Table 3: Training times for a single SAE and one experiment run for ensembles with 8 SAEs on a H100 GPU.

	GELU-1L	Pythia-160M	Gemma 2-2B
Single SAE	3h 2m	5h 43m	11h 7m
Naive Bagging	24h 16m	45h 44m	3d 16h 56m
Boosting	32h 26m	48h 17m	5d 5h 26m

<sup>5</sup><https://pytorch.org/>

<sup>6</sup><https://github.com/jbloomAus/SAELens/tree/main>

Supplementary Table 4: Selected hyperparameter values for the base SAE. These hyperparameters are held constant for all SAEs in the ensemble.

Language Model	Learning Rate	Expansion Factor	TopK	Sparsity Coefficient
GELU-1L	0.0003	32	–	0.75
Pythia-160M	0.0003	21	128	–
Gemma 2-2B	0.0003	7	–	0.75

---

**Algorithm 1:** Training algorithm for the  $j$ th iteration of boosting. Gradient descent with a mini-batch size of 1 is shown as an illustration.

---

**Input:** Training activations  $\{\mathbf{a}^{(n)}\}_{n=1}^N$ , learning rate  $\alpha$ , sparsity coefficient  $\lambda$ , sparsity norm coefficient  $p$ , activation function  $h(\cdot)$ , previous SAEs  $[g(\cdot; \theta^{(1)}), \dots, g(\cdot; \theta^{(j-1)})]$

**Output:** Trained SAE  $g(\cdot; \theta^{(j)})$

```

// Randomly initialize weights
initialize parameters  $\theta^{(j)}$  (i.e.  $\mathbf{W}_{\text{enc}}^{(j)}, \mathbf{b}_{\text{enc}}^{(j)}, \mathbf{W}_{\text{dec}}^{(j)}, \mathbf{b}_{\text{dec}}^{(j)}$ )
initialize  $n = 0$ 
while  $n < N$  do
    // Determine residual from previous SAEs
    initialize  $\mathbf{e} = \text{zeros\_like}(\mathbf{a}^{(n)})$ 
    for  $\ell \in [j - 1]$  do
        | update  $\mathbf{e} \leftarrow \mathbf{e} + g(\mathbf{a}^{(n)} - \mathbf{e}; \theta^{(\ell)})$ 
    end
    // Leftover residual
    set  $\mathbf{r} = \mathbf{a}^{(n)} - \mathbf{e}$ 
    // Determine predicted residual and feature coefficients
    calculate  $\hat{\mathbf{r}} = g(\mathbf{r}; \theta^{(j)})$ 
    calculate  $\mathbf{c} = h(\mathbf{W}_{\text{enc}}^{(j)} \mathbf{r} + \mathbf{b}_{\text{enc}}^{(j)})$ 
    // Calculate loss
    set  $\mathcal{L}_{\text{Boost}}(\mathbf{a}^{(n)}; \theta^{(j)}) = \|\mathbf{r} - \hat{\mathbf{r}}\|_2^2 + \lambda \|\mathbf{c}\|_p$ 
    // Gradient step
    update  $\theta^{(j)} \leftarrow \theta^{(j)} - \alpha \nabla_{\theta^{(j)}} \mathcal{L}_{\text{Boost}}(\mathbf{a}^{(n)}; \theta^{(j)})$ 
    // update  $n$ 
    update  $n \leftarrow n + 1$ 
end

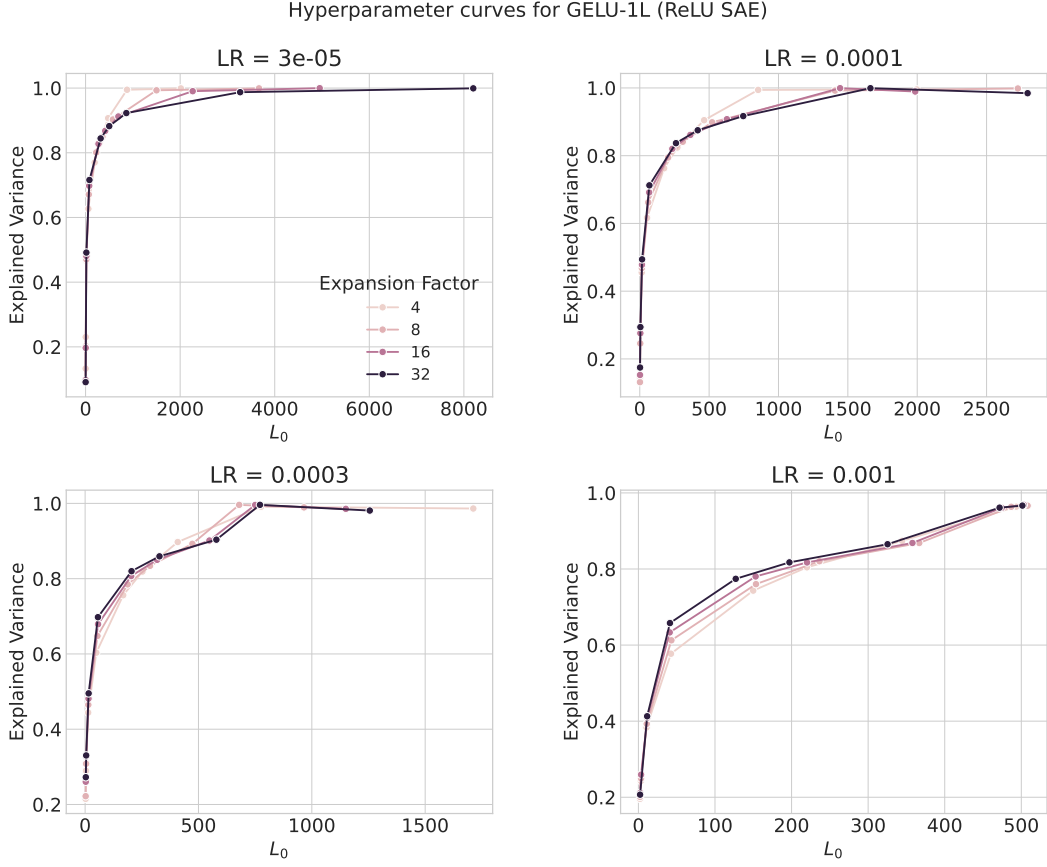
```

---

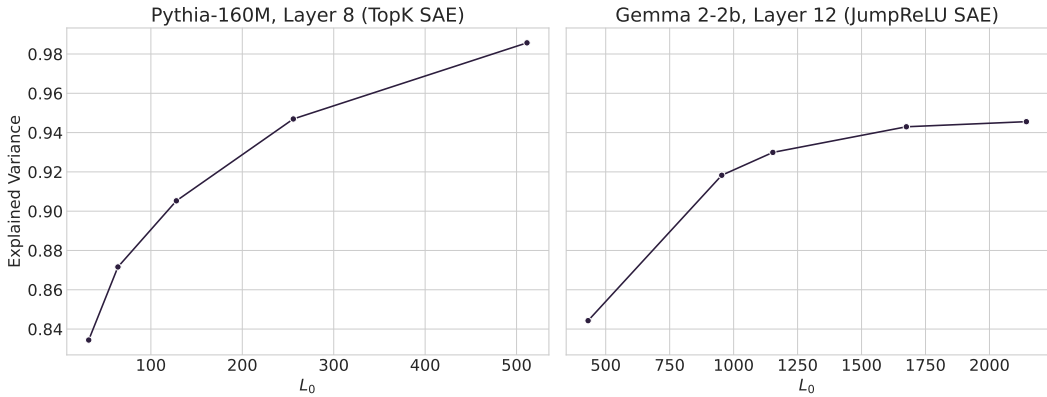
### D.3 Hyperparameter Selection

For the smallest model (GELU-1L), we conduct an extensive hyperparameter search across the learning rate, sparsity coefficient, and the expansion factor (Supplementary Figure 5), where the expansion factor refers to the multiplicative factor for the input activation dimensionality to get the SAE’s hidden dimensionality ( $k = d \times \text{Expansion Factor}$ ). We select the hyperparameters that get closest to 90% explained variance to ensure that the reconstructions are faithful to the original activations.

For the larger Pythia-160M and Gemma 2-2B, we use the same learning rate from GELU-1L and consider expansion factors which give SAEs with a similar dimensionality ( $k$ ) as the SAE for GELU-1L. We perform a sweep over the hyperparameter which controls the sparsity of the SAE (TopK value for Pythia-160M and the  $L_0$  coefficient for Gemma 2-2B) and select the values that give us an explained variance closest to 90% (Supplementary Figure 6). The final selected hyperparameter values are provided in Supplementary Table 4.



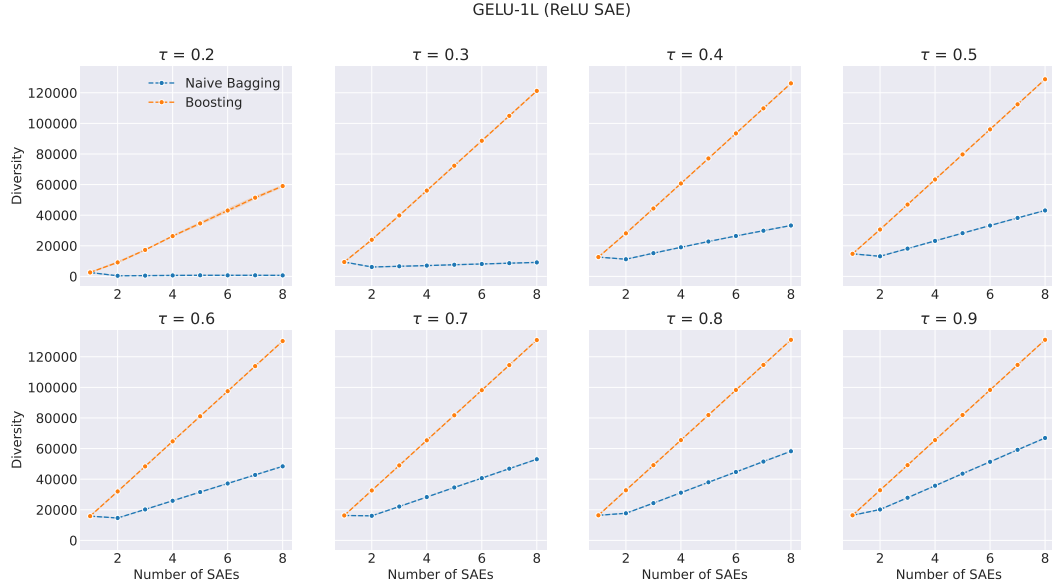
Supplementary Figure 5: Hyperparameter sweep performed for the GELU-1L activations with the ReLU SAE across different learning rates, expansion factors, and sparsity coefficients.



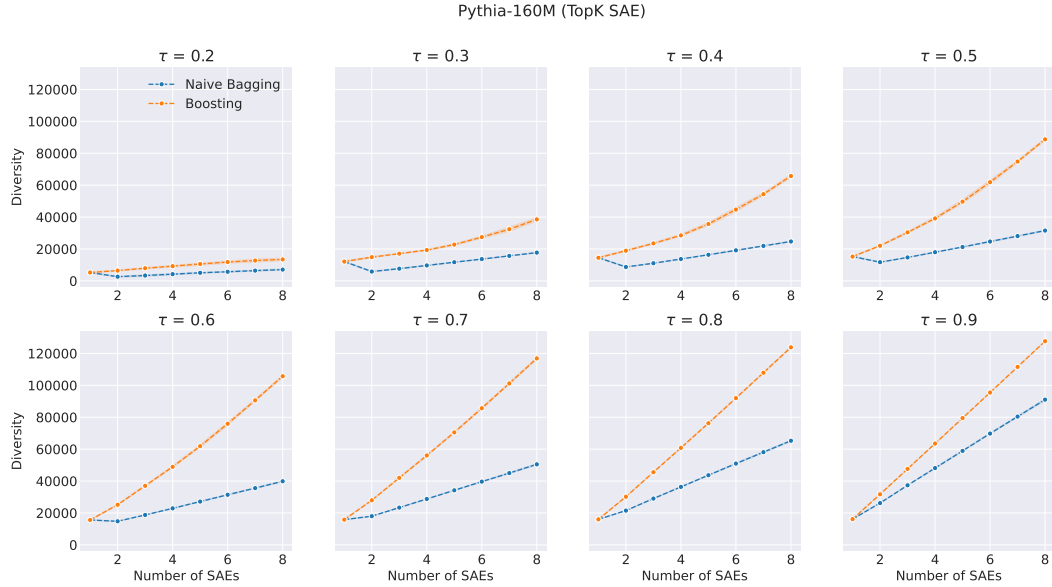
Supplementary Figure 6: Hyperparameter sweep performed for the Pythia-160M and Gemma 2-2B activations with the TopK and JumpReLU SAEs, respectively. For Pythia-160M, the sweep is across different values of  $K$ , and for Gemma 2-2B it is across different sparsity coefficients.

## E Additional Thresholds for Feature Diversity

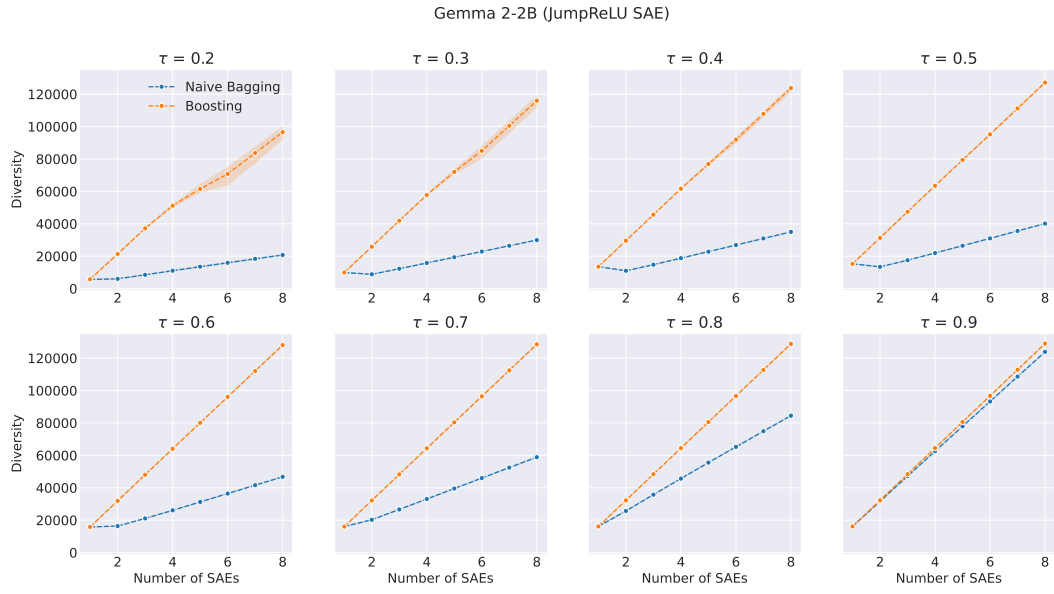
Here we show how the diversity metric changes for different thresholds  $\tau$  (Supplementary Figures 7, 8, 9) with the number of SAEs in the ensemble across all three language models. Overall the trend remains the same as  $\tau = 0.7$ , with boosting learning a higher number of dissimilar features than naive bagging with each added SAE. Also, as expected, a smaller number of diverse features are learned for lower thresholds.



Supplementary Figure 7: Diversity metric evaluation for boosting and naive bagging across various similarity thresholds for GELU-1L. Shaded regions indicate 95% confidence intervals across 5 experiment runs.



Supplementary Figure 8: Diversity metric evaluation for boosting and naive bagging across various similarity thresholds for Pythia-160M. Shaded regions indicate 95% confidence intervals across 5 experiment runs.



Supplementary Figure 9: Diversity metric evaluation for boosting and naive bagging across various similarity thresholds for Gemma 2-2B. Shaded regions indicate 95% confidence intervals across 5 experiment runs.